Temperature and hydrogen diffusion length in hydrogenated amorphous silicon films on glass while scanning with a continuous wave laser at 532 nm wavelength

Wolfhard Beyer (iD), Gudrun Andrä, Joachim Bergmann, Uwe Breuer (iD), Friedhelm Finger, Annett Gawlik, Stefan Haas, Andreas Lambertz, Florian C. Maier, Norbert H. Nickel, and Uwe Zastrow

View Online   Export Citation   CrossMark

ARTICLES YOU MAY BE INTERESTED IN

Temperature and hydrogen diffusion length in hydrogenated amorphous silicon films on glass while scanning with a continuous wave laser at 532 nm wavelength

Wolfhard Beyer,[1,2,a)] Gudrun Andrä,[3] Joachim Bergmann,[3] Uwe Breuer,[4]
Friedhelm Finger,[1] Annett Gawlik,[3] Stefan Haas,[1] Andreas Lambertz,[1] Florian C. Maier,[1]
Norbert H. Nickel,[2] and Uwe Zastrow[1]

[1]*IEK-5 Photovoltaik, Forschungszentrum Jülich GmbH, D-52425 Jülich, Germany*
[2]*Institut für Silizium-Photovoltaik, Helmholtz-Zentrum Berlin für Materialien und Energie GmbH, Kekuléstraße 5, D-12489 Berlin, Germany*
[3]*Photovoltaische Systeme, Leibniz-Institut für Photonische Technologien e.V., Albert-Einstein-Straße 9, D-07702 Jena, Germany*
[4]*ZEA-3 Analytik, Forschungszentrum Jülich GmbH, D-52425 Jülich, Germany*

Rapid thermal annealing by, e.g., laser scanning of hydrogenated amorphous silicon (a-Si:H) films is of interest for device improvement and for development of new device structures for solar cell and large area display application. For well controlled annealing of such multilayers, precise knowledge of temperature and/or hydrogen diffusion length in the heated material is required but unavailable so far. In this study, we explore the use of deuterium (D) and hydrogen (H) interdiffusion during laser scanning (employing a continuous wave laser at 532 nm wavelength) to characterize both quantities. The evaluation of temperature from hydrogen diffusion data requires knowledge of the high temperature (T > 500 °C) deuterium-hydrogen (D-H) interdiffusion Arrhenius parameters for which, however, no experimental data exist. Using data based on recent model considerations, we find for laser scanning of single films on glass substrates a broad scale agreement with experimental temperature data obtained by measuring the silicon melting point and with calculated data using a physical model as well as published work. Since D-H interdiffusion measures hydrogen diffusion length and temperature within the silicon films by a memory effect, the method is capable of determining both quantities precisely also in multilayer structures, as is demonstrated for films underneath metal contacts. Several applications are discussed. Employing literature data of laser-induced temperature rise, laser scanning is used to measure the H diffusion coefficient at T > 500 °C in a-Si:H. The model-based high temperature hydrogen diffusion parameters are confirmed with important implications for the understanding of hydrogen diffusion in the amorphous silicon material. *Published by AIP Publishing.* https://doi.org/10.1063/1.5038090

I. INTRODUCTION

Annealing (thermal treatment) of hydrogenated amorphous silicon (a-Si:H) films and corresponding materials is of interest for changing and improving material and device properties. For example, hydrogen diffusion caused by an enhanced temperature may lead to saturation of silicon dangling bonds in the bulk a-Si:H material or at its surfaces/interfaces resulting in improved device properties. Furthermore, hydrogen outdiffusion from a-Si:H based surface layers on crystalline silicon (c-Si) may passivate c-Si defects at surfaces or in bulk. Indeed, improvement of films and devices based on a-Si:H and related materials by annealing is well known: (i) light-induced defects in a-Si:H are known to anneal out near 150 °C,[1] (ii) amorphous silicon based solar cells deposited at the rather low temperature of 120 °C improved considerably when annealed at T = 120 °C

for up to 2 h,[2] (iii) silicon heterojunction solar cells with thin layers of a-Si:H on top of crystalline silicon have been reported to require an annealing step near 180 °C to reach high carrier lifetime at the c-Si surface and high conversion efficiencies,[3] and (iv) hydrogenated silicon nitride films on multicrystalline silicon solar cells have been found to reduce the light-induced degradation in these solar cells when annealed near 700-800 °C.[4] Annealing of a-Si:H is also of interest for driving out hydrogen for subsequent laser crystallization,[5–9] as in laser crystallization processes the presence of hydrogen in amounts of about 10 at. % can complicate the crystallization[9] and can cause bubble formation,[10] explosive hydrogen evolution,[11,12] and film ablation.[13] A total dehydrogenization of the films, however, was found to be unnecessary[11] and not desirable as H is required in the (crystallized) polycrystalline silicon for grain boundary passivation.[11,14]

The standard technique for annealing uses a furnace with the advantage of well-known annealing temperature and annealing time. However, furnace annealing is often too time consuming or too expensive for device production or cannot

a)Author to whom correspondence should be addressed: w.beyer@fz-juelich.de

be applied because parts of a device may not survive the annealing procedure. Short-term annealing by rapid thermal processing (RTP) methods (which include heating by optical illumination, laser beams, laser pulses, and others) may be an alternative to furnace annealing, because process time can be reduced and heating can be confined to thin surface layers. Indeed, excimer laser annealing is now widely used in low temperature polycrystalline silicon thin film transistor technology on glass[6] for large area display application, and, recently, efficient crystallized silicon solar cells were obtained by liquid phase crystallization using laser scanning.[15] Besides possibilities of depth-dependent heating,[11] RTP/laser annealing methods also allow for a spatially resolved heat treatment. For example, Mei *et al.*[16,17] reported spatially resolved laser annealing for application in thin film transistor technology. For solar cell fabrication, this latter technique may also open new manufacturing options.

Although laser annealing without crystallization was applied to hydrogenated amorphous silicon as early as 1979[18] and there was intensive work on laser crystallization of amorphous silicon,[5–17,19] rapid thermal annealing (including laser annealing) without intentional crystallization is, to our knowledge, not widely applied in silicon technology so far. For dehydrogenation of a-Si:H films targeting subsequent crystallization, multistep laser treatments were proposed.[5,14,16,17] In these experiments, however, the decrease in H concentration overlapped with the increase in crystallinity so that no a-Si:H with reduced H concentration was identified. With regard to defect reduction/device improvement by laser annealing, only a few reports have been published like studies by Lee *et al.*[20] and Chowdhury *et al.*[21] who indeed found improvement of amorphous and polycrystalline silicon based devices by laser treatment. One reason for the limited application may be the lack of knowledge of the precise temperature as in practice the absolute temperature for RTP is often unknown[22] and the effort to measure the RTP temperature accurately by conventional methods (like thermal imaging camera,[21] pyrometer,[23] or thermocouple[24]) is clearly high.

On the other hand, for a simple continuous wave (cw) laser heating of homogeneous material or of thin films on a homogeneous substrate material, the temperature in the laser spot can be readily obtained by mathematics, i.e., by solving the heat diffusion equation (Carslaw and Jaeger[25]) or by applying corresponding computer programs. Indeed, numerous basic studies applicable to the present laser setup (cw laser with the Gaussian intensity profile) exist,[26–29] and based on this, the temperature for the simple setup of a thin film on a substrate can be calculated for known or estimated thermal parameters of the thin film and the substrate. However, calculation of temperature gets more difficult if one is dealing with several layers[30–32] on a substrate, as is the case in thin film silicon solar cells on glass substrates involving metal or transparent conducting oxide contact films. Calculation gets practically impossible if the interfaces between individual films and between films and the substrate have a poor quality. Indeed, when we started our study aiming to apply laser annealing to films of hydrogenated amorphous silicon and thin film silicon solar cells, a multitude of films deposited on various substrates were destroyed under pre-calculated laser treatment conditions, i.e., formed bubbles or peeled off. The peeling of thin film silicon on substrates can have several reasons like internal/external stress, poor interfaces, hydrogen accumulation in bubbles, etc.[33,34] Hence, it became apparent that it was necessary to measure the temperature which the actual film (even if partly destroyed) had encountered, since impeded heat flow, e.g., at defective interfaces between film and substrate or by a poor thermal contact between small laser-treated samples and a heat sink, can raise the actual film surface temperature greatly. Thus, it was expected that by a reliable measurement of the temperature in the laser spot, any interface or heat sink problem could be identified and solved.

From previous work on hydrogen diffusion in a-Si:H,[35,36] it was known that in the latter material (when deposited with a dense/compact structure), hydrogen migration is highly sensitive to temperature and it was expected, therefore, that hydrogen diffusion during laser treatment could be used as a memory effect for temperature characterization. For this purpose, we studied the effect of laser treatment on a-Si:H films of various thicknesses, deposited on different types of substrates. The aim was to explore, whether, and to what extent hydrogen diffusion (outdiffusion and interdiffusion) can deliver the temperature which a laser-treated a-Si:H film has encountered. First results obtained for a-Si:H films deposited on crystalline silicon substrates were published elsewhere.[37] It was found (by monitoring silicon crystallization) that, in particular, interdiffusion of deuterium and hydrogen has a high potential for precise measurements of the laser spot temperature in a certain temperature range and that by careful interface treatments including the application of thin interface layers, the bubbling and peeling effects can be largely avoided.[37]

In this article, results of laser annealing of (dense) undoped a-Si:H films on Corning Eagle glass[38] are discussed. While a rather specific substrate and a specific laser scanning method were used, we note that various issues of the present work are more general. For example, the temperature measurement by the D-H interdiffusion method can be done on films deposited on any type of substrate and with any cw laser scanning conditions, as long as a laser residence time/annealing time[37] can be defined and a certain temperature range is reached. The D-H interdiffusion analysis for temperature measurement is also expected to work for conventional RTP with known heating time. Thus, this method may provide temperature/process information for many types of rapid thermal processing of hydrogenated amorphous silicon and related materials. The method is not even confined to hydrogenated materials, as, e.g., ion implantation may be used for hydrogen (and deuterium) incorporation. However, it is necessary for a successful application of the D-H method that H diffusion increases strongly with rising temperature as is the case for compact a-Si:H.[35,36] This strong temperature dependence of H diffusion causes that the distributions of deuterium and hydrogen in the films are frozen in rapidly when the laser beam moves on. At a later time, the distributions of deuterium and hydrogen can be analyzed by, e.g., secondary ion mass spectrometry (SIMS)

measurements. A strong temperature dependence of H diffusion, i.e., an Arrhenius dependence with diffusion energies exceeding about 1 eV, has been found, besides for films of a-Si:H, e.g., for films of microcrystalline silicon,[39] hydrogen implanted single crystalline silicon,[40] hydrogenated amorphous germanium,[41,42] hydrogenated stoichiometric silicon nitride,[43,44] silicon oxynitride,[44] as well as zinc oxide.[45]

Since the measurement of the temperature in the laser spot by the D-H interdiffusion method involves models and assumptions,[37] we undertook a broad scale effort to compare the D-H interdiffusion results with data on the temperature in the laser spot obtained by other methods: (i) we determined the temperature by measuring the laser power necessary for melting,[46] (ii) we estimated the temperature by applying a physical model, and (iii) we used published data on the temperature rise based on temperature calculations.[27,28] For these comparisons, we used a simple laser annealing setup with single amorphous silicon films (a-Si:H/a-Si:D double layers) grown on glass substrates[38] with optimized interface conditions. A good agreement is found, also confirming that in this simple case, the temperature in the laser spot can directly be inferred from the laser scanning parameters if the thermal properties of the substrate material (heat diffusivity and heat conductivity) are known. For a more complicated setup like laser scanning of films absorbing laser light underneath metal contacts, i.e., when temperature calculation is difficult, we expect and find that the D-H interdiffusion method is still applicable.

By measuring deuterium and hydrogen interdiffusion in dense a-Si:H, information is directly gained on the hydrogen diffusion length. Since most annealing processes in a-Si:H are likely based on hydrogen diffusion,[47,48] the hydrogen diffusion length must be considered as the primary quantity characterizing an annealing procedure. This is supported for our a-Si:H material by the observation that a fixed photodarkening effect[18] corresponds to a fixed H diffusion length for a given film. The hydrogen diffusion length L, the temperature dependent (strongly with T rising) H diffusion coefficient D (T), and the annealing time t are interconnected by the relation $L = 2 [D(T) t]^{1/2}$. Accordingly, the same annealing effects (corresponding to a specific H diffusion length) as observed for furnace annealing in the $T \leq 500\,°C$ range (using annealing time periods ≥ 5 min) are expected to occur for RTP at a much higher temperature due to the much shorter annealing time periods. The equivalent temperatures for RTP and furnace annealing (leading to the same H diffusion lengths) are defined by the different annealing time periods if D(T) is known. Experimental data of D(T) for D-H interdiffusion are available so far only up to $T = 500\,°C$,[35,36] limited by extensive H outdiffusion and crystallization at higher T. As D(T) at $T > 500\,°C$ is required in this work, we used model values.[35–37] Since H diffusion depends on the H chemical potential which is known to decrease on H outdiffusion,[35] H diffusion data based on H effusion[49] (which involves much H outdiffusion) cannot be used and we confine here entirely on D-H interdiffusion data with little H outdiffusion.[35] Laser annealing related D-H interdiffusion and temperature calculation[27] open the possibility to measure the (D-H interdiffusion based) H diffusion coefficient at a much higher temperature than available so far, due to the dependence of crystallization temperature on annealing time[50] and due to the short annealing time periods involved in laser scanning. The upper limit of D-H interdiffusion-based H diffusion data is extended in this work by more than 300 °C up to $T > 800\,°C$. The results confirm the model assumptions for high temperature H diffusion, contributing to the understanding of the Meyer-Neldel rule and of the time-dependence of H diffusion in a-Si:H.[35,36]

II. EXPERIMENTAL DETAILS

Laser scanning was applied to device-grade (undoped) a-Si:H films fabricated by plasma deposition on glass plates (Corning Eagle;[38] thickness 1 mm; area 10×10 cm^2). A layer of deuterated amorphous silicon (a-Si:D) with a thickness of approximately $0.05\,\mu$m was deposited onto the a-Si:H which had (approximate) layer thicknesses of $0.3\,\mu$m (sample L24) and $0.7\,\mu$m (sample L12). The deposition temperature of both hydrogenated and deuterated a-Si films was about 185 °C. The concentration of silicon-bonded hydrogen/deuterium in this material measured by infrared absorption is approximately 15 at. %. Hydrogenated amorphous silicon deposited under these conditions is used in thin film silicon solar cells,[51] and from previous work, it is known that it is a rather dense (compact) material with the diffusion of hydrogen predominantly by atoms and not by molecules.[35,36] We measured deuterium-hydrogen interdiffusion by secondary ion mass spectrometry (SIMS) profiling.[35–37,52] A time of flight instrument (TOFSIMS-IV, Iontof GmbH, Münster, Germany) was applied. An area of $300 \times 300\,\mu$m^2 was sputtered (using a Cs ion beam), and an area of approximately $80 \times 80\,\mu$m^2 was measured (using a Bi$_3$ ion beam). For laser scanning, a Coherent Verdi laser with a wavelength of 532 nm and nominally 6.5 W optical power was used. This light is almost fully absorbed at a depth of $0.1\,\mu$m. A circular Gaussian laser spot of S = 0.7 mm in diameter (defined by a 1/e reduction of laser intensity) was scanned over fields of 9 mm × 9 mm at scanning speeds v between 1 and 100 mm/s with a line offset of 0.35 mm. Various levels of laser power (≤ 6 W giving rise to energy flow densities < 1.6 kJ/cm^2 s) were applied. Laser scanning was performed from the glass side, from the a-Si:H layer side, as well as from the glass side into an a-Si:H layer with silver metallization, as shown schematically in Fig. 1(a). The transmitted light image (illumination with white light) of sample L24 after laser scanning is shown in Fig. 1(b). The values in the first line in each 1 cm × 1 cm field (marked by laser scribing) give the nominal laser power (in watts), the values in the second line indicate the scanning speed (i.e., v5 means a velocity of 5 mm/s), and the letters G and L indicate laser irradiation from glass and a-Si:H layer sides, respectively. The black areas in the lower part of the glass plate are covered with silver metallization and thus are not transparent. The a-Si:H film in Fig. 1(b) has a brown color with different darkening stages. This various darkening of the amorphous Si film after laser scanning is attributed to H outdiffusion causing a reduction of the bandgap of a-Si:H[18] and thus to an enhanced light absorption. The presence of (solid phase) crystallized silicon shows
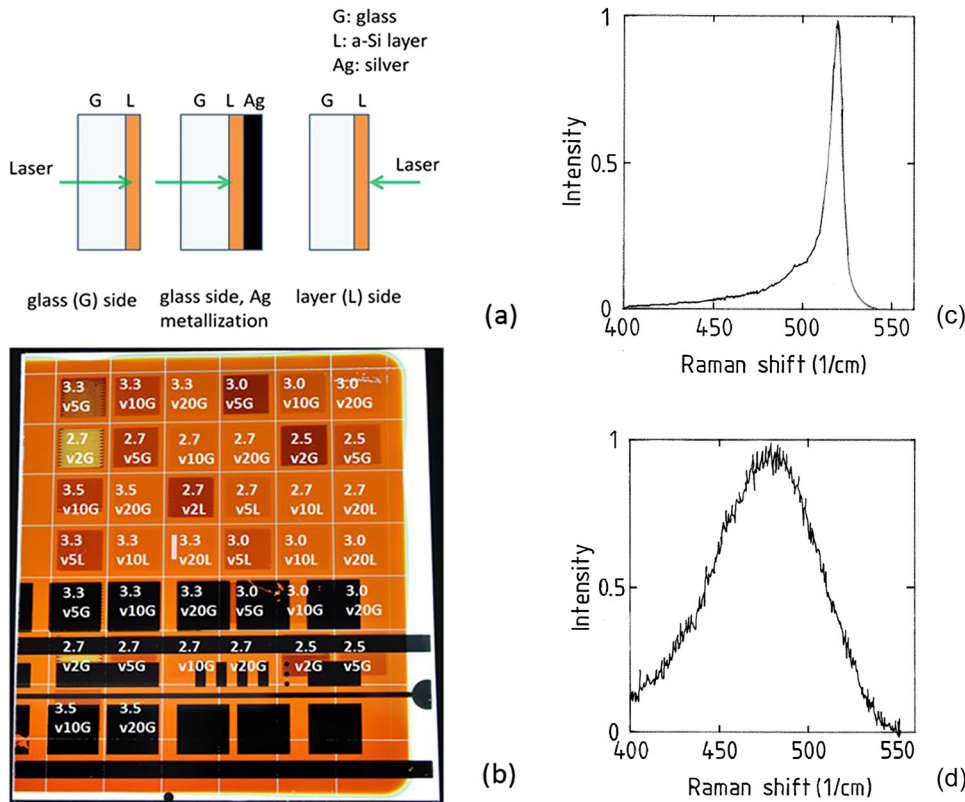
FIG. 1. Schematic setup for laser treatment of the a-Si:H layer on glass (a), transmitted light image of glass plate L24 coated with $0.3\,\mu m$ a-Si:H and $0.05\,\mu m$ a-Si:D, scanned at various laser power and scan speed values (see text) (b), Raman scattering spectrum of crystallized silicon (in field 3.3/v5G) (c) and of amorphous silicon (in field 3.3/v10G) (d).

up by a yellow color in some fields. As an example, the Raman spectrum of Fig. 1(c) measured in the yellow area of field 3.3/v5G shows a typically crystalline silicon signature, while the spectrum in Fig. 1(d) measured in field 3.3/v10G (having brown color) shows fully amorphous behavior.[53] After laser scanning, the glass plate was cut into pieces of about 1×1 cm^2 area used for sample analysis.

We note that our laser scanning conditions, in particular the use of a Gaussian intensity profile, lead to quite inhomogeneous irradiation perpendicular to the scan direction (see Sec. III K). We chose these conditions primarily because laser scanning with the Gaussian intensity profile is the historical standard technique with numerous basic studies,[27–30,32] and thus, a comparison with previous work, in particular with temperature calculations,[27,28] is readily possible (see Sec. III G). The main target of the present work, the demonstration that D-H interdiffusion can be used for precise measurement of H diffusion length and temperature in the laser spot in (a-Si:H based) multilayer films on glass, is not affected by this inhomogeneity. Irradiation with higher homogeneity is achievable by, e.g., multiple scans with a circular Gaussian intensity profile, scans with flat-top (top hat) intensity profiles,[31] scans with line lasers,[21] or applying conventional RTP.

III. RESULTS AND DISCUSSION

A. Measurement of hydrogen diffusion length and temperature in the laser spot by D-H interdiffusion

Typical SIMS depth profiles prior to (a) and after (b) laser scanning are shown in Fig. 2. The SIMS signals (SIMS intensity) of several masses versus sputter time t_s are plotted. The spreading of the deuterium into the hydrogenated

material after laser scanning is visible. Some outdiffusion of hydrogen towards the film surface and the film-glass interface (the latter involved a thin vacuum-deposited SiO$_2$ interlayer) is also visible, as expected for heating of thin a-Si:H layers.[49] By depth profiling of the SIMS sputtering craters, the sputter time scale can be converted to a depth scale. The deuterium [D/(D + H)] depth profiles were then fitted by complementary error functions as solutions of the diffusion equation. The fit yields directly the hydrogen diffusion length L.[52]

To evaluate the annealing temperature from the H diffusion length, we determined first the hydrogen diffusion coefficient D during laser treatment by employing the definition of diffusion length, $L = 2(D\,t)^{1/2}$ and using for the annealing time t the laser beam residence time $t^* = S/v$ (S is the laser spot diameter and v is the scan velocity). For the second step, namely, the derivation of the temperature from the H diffusion coefficient, the temperature dependence of the (D-H interdiffusion-based) H diffusion coefficient, D(T), needs to be known in a temperature and H diffusion coefficient range, where no experimental data exist so far. Note that the H diffusion coefficients observed in the present laser annealing experiment are typically in the range of 10^{-11}–10^{-9} cm^2 s^{-1}, i.e., much higher than observed for furnace annealing ($\leq 10^{-12}$ cm^2 s^{-1} at T ≤ 500 °C).[35] However, model concepts for high temperature H diffusion in a-Si:H exist[35–37] and these are used. Since hydrogen diffusion in dense a-Si:H generally follows Arrhenius temperature dependences,[35,36,52] i.e., D(T) = D$_0$ exp(−E$_D$/kT) (k is the Boltzmann constant), D(T) can be characterized by the diffusion energy E$_D$ and the diffusion prefactor D$_0$. While the temperature dependence of H diffusion in a-Si:H at temperatures <500 °C is known to vary with hydrogen concentration
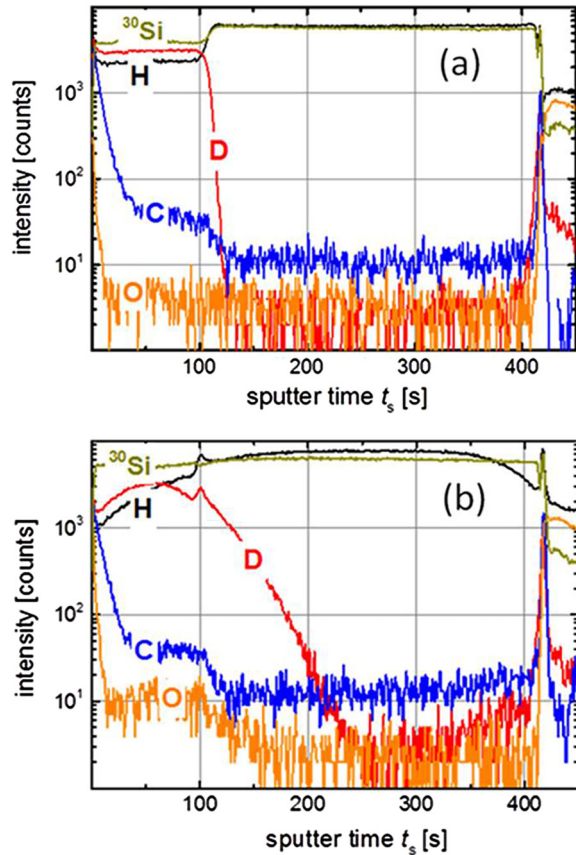
FIG. 2. SIMS profiles of the D-H sandwich sample (L24, $0.3\,\mu$m a-Si:H layer thickness) prior to (a) and after (b) laser scanning with 3.0 W, 10 mm/s from glass side (field 3.0/v10G in Fig. 1). Several masses are plotted as a function of sputtering time t_s. H refers to the hydrogen isotope ^{1}H (atomic mass 1) and D to the hydrogen isotope ^{2}H (deuterium, atomic mass 2).

and other parameters, a Meyer-Neldel dependence has been reported by Shinar *et al.*[54] and by Beyer[35,36] for D_0 and E_D. This implies that at the Meyer-Neldel temperature T^{MN}, all (extrapolated) H diffusion coefficients meet. For the Meyer-Neldel dependence $D_0 = D^{MN} \exp(E_D/kT^{MN})$ of
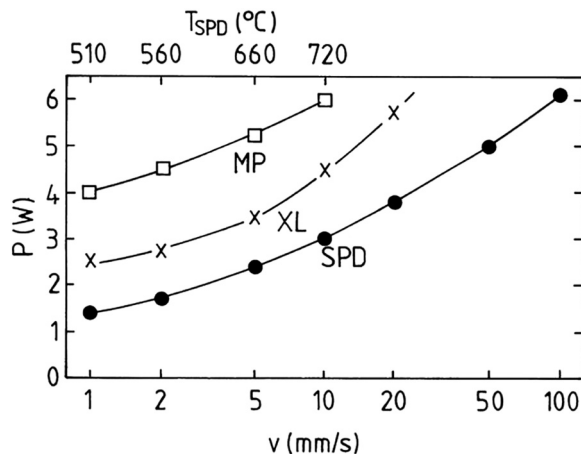

FIG. 3. Empirical relation between laser power P (illumination from glass side) and scan speed v for the silicon melting point (MP), the solid phase crystallization (XL), and the standard photo-darkening (SPD). Also given in the upper part of the figure are the temperatures T_{SPD} which correspond to the standard photo-darkening.

undoped a-Si:H, the parameters $D^{MN} \approx 6 \times 10^{-13}\,\mathrm{cm^2\,s^{-1}}$ and $T^{MN} \approx 760\,\mathrm{K}$ were evaluated by Ref. 35. Reference 54 reported $T^{MN} \approx 730\,\mathrm{K}$. Thus, the temperatures in the laser spot encountered in this study are mostly equal or exceeding T^{MN}. Hydrogen diffusion in a-Si:H was described by Beyer[35,36] in terms of chemical reactions which define the concentration of diffusing (i.e., non-trapped) hydrogen in a transport path. The occurrence of a Meyer-Neldel rule for H diffusion was attributed to non-equilibrium/extrinsic effects in H diffusion at lower temperature changing to an equilibrium situation near the Meyer-Neldel temperature. This explanation of the observed Meyer-Neldel rule suggests that the H diffusion coefficient at temperatures exceeding T^{MN} should follow a rather well defined Arrhenius temperature dependence unaffected by H concentration. Assuming that the hydrogen diffusion prefactor D_0 is given by the theoretical diffusion prefactor of silicon ($D_0^T = v_{ph}\,a^2/6 \approx 10^{-3}\,\mathrm{cm^2\,s^{-1}}$ with the hopping distance $a \approx 2.5\,\text{Å}$ and the phonon frequency $v_{ph} \approx 10^{13}\,\mathrm{s^{-1}}$), a diffusion energy $E_D \approx 1.39$ eV was evaluated.[35] These latter H diffusion parameters D_0 and E_D were used in the present article as well as in previous work[37] to characterize the Arrhenius dependence D(T) necessary for the evaluation of the H diffusion temperatures from the measured H diffusion coefficients in the high temperature range. As discussed in Sec. III I, the measured high temperature hydrogen diffusion data presented in this article are consistent with these model-based H diffusion parameters. We note that the light-enhanced hydrogen motion described by Santos *et al.*[55] is too small in the temperature range of focus to affect the H diffusion processes.

B. Temperature evaluation based on silicon melting point analysis

For the measurement of temperature in the laser spot by the melting point (MP) analysis,[46] we assume a linear relation between temperature and the applied laser power up to the silicon melting temperature, based on earlier work.[18,26] We neglect here minor deviations expected due to changes of thermal conductivity, reflectivity, etc. as a function of temperature. By associating for a given scan speed the laser power resulting in the melting of the silicon film with a temperature of 1414 °C (the melting point of silicon), the temperature corresponding to any lower laser power at the same scan speed follows. Figure 3 shows for sample L12 the laser power P which needs to be applied (from the glass side) to reach the melting point (MP). For the scan speeds of 1, 2, 5, and 10 mm/s, the laser power P_{MP} values of 4.0, 4.5, 5.25, and 6 W, respectively, were determined. Since the available laser power was limited to 6.5 W, for the applied scan speeds >10 mm/s the laser power for film melting could not be measured.

The laser power values for the solid phase crystallization (XL) and the "standard photo-darkening" (SPD) as a function of scan speed v are also shown in Fig. 3. We define the standard photo-darkening by a just clearly visible reduction of transmitted light intensity, well aware that this definition appears rather subjective. Therefore, measurements of light transmission were performed showing that this clearly visible reduction of transmitted (white) light intensity corresponds to

a change of transmitted light intensity at 600 nm by a factor of 0.7-0.8. Note that photo-darkening[18] is of interest as a rapid way for characterization of the annealing state of a-Si:H films. For all selected threshold processes, i.e., melting, solid phase crystallization, and photo-darkening, the respective laser power was determined by analyzing scan lines using microscopic inspection (molten Si re-crystallizes to large crystallites exceeding $1\,\mu m$ in size). To determine any temperature T for a given scan speed v and laser power P (v), we used the formula

$$T(v) = 20\,^\circ C + \frac{P(v)(1414\,^\circ C - 20\,^\circ C)}{P_{MP}(v)}, \qquad (1)$$

accounting for room temperature ($20\,^\circ C$) as the reference temperature for all laser-induced temperature enhancement. The temperatures T_{SPD} for the standard photo-darkening thus calculated are given in the upper part of Fig. 3. It should be mentioned that the accuracy of the melting threshold power P_{MP} is in the range of $\pm 10\%$ and may get influenced additionally by the formation of bubbles in the a-Si:H films at temperatures near the melting point.

Figure 4 shows the transmitted light image (illumination with white light) of the part of sample L12 which was evaluated by SIMS measurements of D-H interdiffusion. Some laser scan lines applied for measuring the data of Fig. 3 are visible in the upper part. For the individual fields, the applied laser scan speed and laser power are indicated. Note that the laser power values for sample L12 were chosen with the aim to obtain a constant photo-darkening PD for various scan speeds. Laser power values P (v) = PD × P_{SPD} (v) were applied, using P_{SPD} (v) values of Fig. 3.

C. Comparison of temperatures evaluated by the two experimental methods

Figure 5 shows for sample L12 the temperature T_{DH} obtained by D-H interdiffusion plotted as a function of the
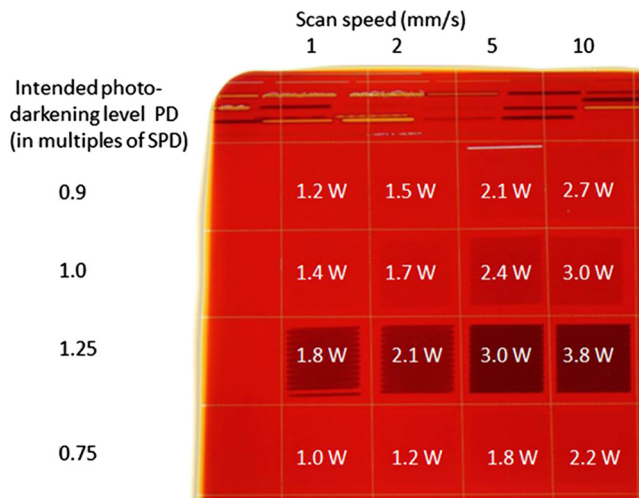

FIG. 4. Transmitted light image of a fraction of sample L12 (a-Si:H/D thickness $0.75\,\mu m$) treated by laser scanning (glass side) using four scan speeds and various laser power values as indicated within the fields. Laser power was chosen according to Fig. 3 aiming to obtain certain darkening levels PD as indicated on the left side.
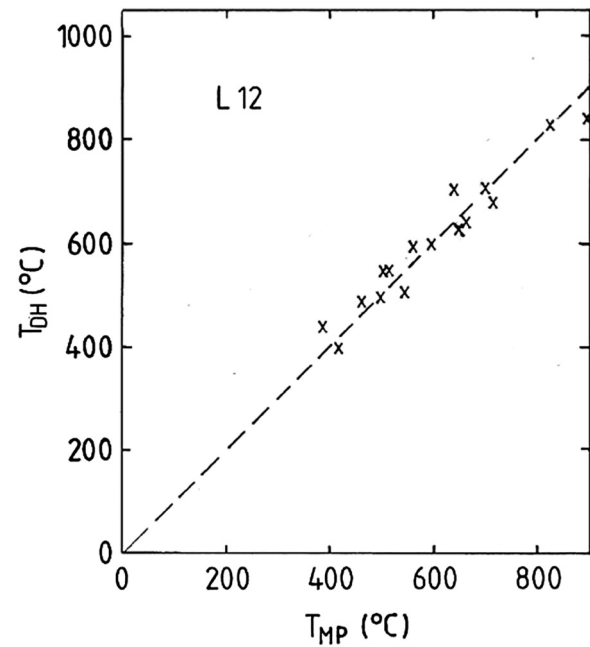

FIG. 5. Temperature T_{DH} determined by D-H interdiffusion versus temperature T_{MP} determined by comparison of the used laser power with the power required for melting of the silicon film. All data points refer to sample L12 and to scan velocities between 1 and 10 mm/s. Dashed line: $T_{DH} = T_{MP}$.

temperature T_{MP} obtained by using Eq. (1) and the laser power values of Fig. 4. The data refer to illumination from the glass side. Although some scattering is observed, the results demonstrate that the two temperatures agree on the average, supporting the assumptions made. In particular, this agreement supports the assumptions made for the high temperature H diffusion parameters. Also, the assumption that the annealing time t equals the laser residence time t* (i.e., laser spot diameter divided by scan speed) is confirmed by the agreement of the temperatures obtained by the two methods: this assumption enters the evaluation of D-H interdiffusion while for the melting point method no such assumption is required. For the Gaussian laser spot applied, both methods of temperature measurements are considered to refer rather to the maximum temperature than to the average temperature within the laser spot. This is due to the exponential (strong) temperature dependence of the hydrogen diffusion coefficient,[35,36] the rather small sampling size of the SIMS instrument, the SIMS measurements performed predominantly in areas of highest photo-darkening, and because the optical inspection of laser-induced melting is most sensitive to the highest temperature.

D. Relationship between hydrogen diffusion length and photo-darkening effect

In Fig. 6, the hydrogen diffusion length L determined by D-H interdiffusion is plotted as a function of scan speed v for various laser-treated fields of sample L12 (see Sec. III B, Fig. 4). The results show quite constant H diffusion lengths (independent of scan speed) for fixed photo-darkening levels in agreement with the assignment of the photo-darkening effect to H outdiffusion.[18] The successful characterization of
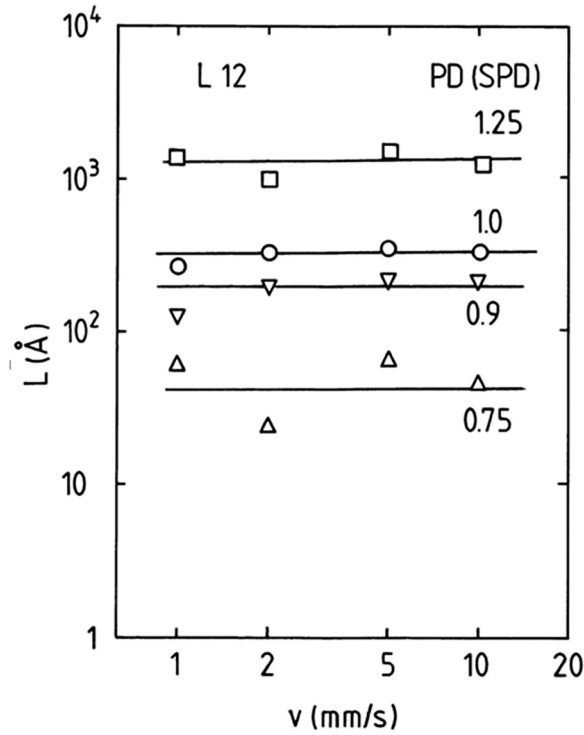
FIG. 6. Hydrogen diffusion length L in sample L12 as a function of laser scan speed v for various (intended) photo-darkening (PD) levels.

FIG. 8. Temperature T_{DH} in the laser spot as a function of (nominal) laser power P and scan speed v for samples L12 (open symbols) and L24 (closed symbols). Illumination was from the glass side.

the annealing (photo-darkening) state by the hydrogen diffusion length, as expected for H diffusion related annealing is here directly seen. Figure 7 shows the photo-darkening PD as a function of H diffusion length L for sample L12 based on the data of Fig. 6. The straight line indicates the dependence PD $\approx$ 0.33 log L + 0.2. Note, however, that the H diffusion length measures the hydrogen diffusion in the bulk material near the D/H interface, while the photo-darkening effect involves the (H outdiffusion related) hydrogen distribution
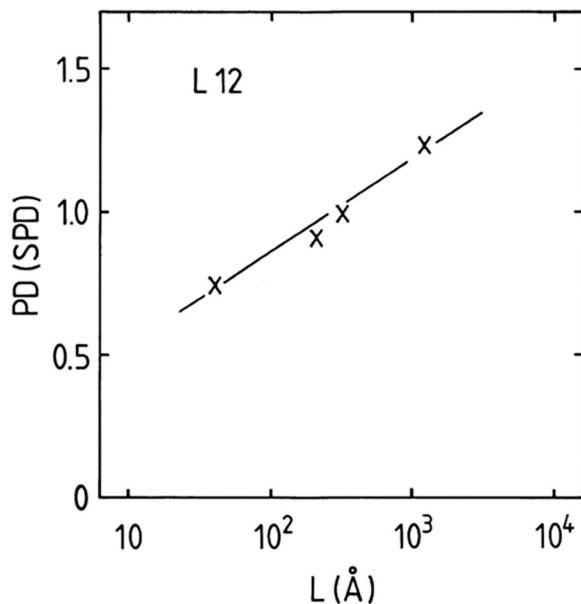

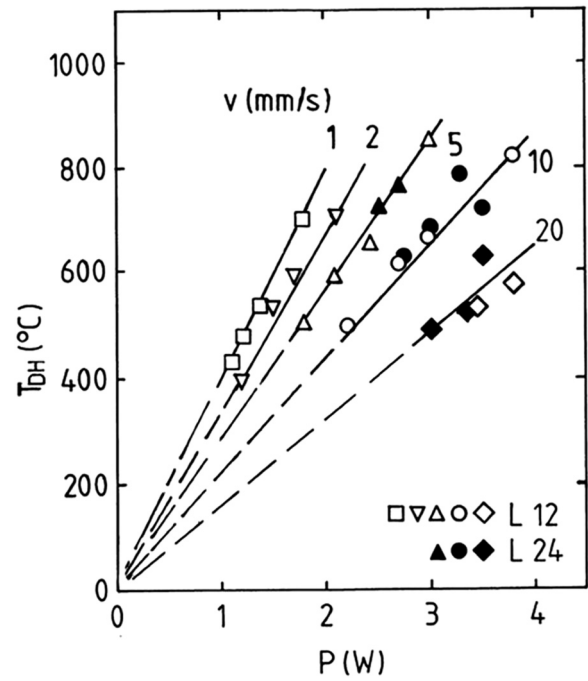FIG. 7. Photo-darkening PD as a function of hydrogen diffusion length L (sample L12).

over the whole film thickness[37] and its influence on light transmission. Therefore, the dependence on Fig. 7 cannot be universal but is expected to be affected, e.g., by film thickness.

By the same reason, a direct relationship between the optical absorption of an a-Si:H film and the annealing temperature as discussed by Ance *et al.*[56] cannot be generally valid. It is ignored that H outdiffusion can generate quite different depth profiles of hydrogen concentration, depending strongly on the a-Si:H material structure (compact or void-rich material) and on the properties of the film surface and the film-substrate interface.[37,57,58] Conclusions from optical (absorption) measurements toward the annealing temperature appear only possible if the depth dependence of the hydrogen concentration (or of the optical bandgap) is measured in the annealed state. Indeed, evaluation of hydrogen outdiffusion depth profiles (for rather small H diffusion lengths) may be an alternative way to determine the H diffusion coefficient[37,58] and thus the temperature in the laser spot (see Sec. III A) without the need of deuterated layers.

E. Influence of laser scan speed and film thickness

In Fig. 8, the temperature T_{DH} in the laser spot measured by D-H interdiffusion (glass side illumination) is shown as a function of laser power P. The data are consistent with the linear dependence of laser spot temperature on laser power as assumed for the application of the melting point method (see Sec. III B). Note that for P = 0 W, the reference temperature is room temperature (20 °C). T_{DH} in Fig. 8 is seen to depend on laser scan speed v. Since there is no significant difference between results for sample L12 (0.75 μm a-Si thickness) and for sample L24 (0.35 μm a-Si thickness), the temperature in

the laser spot does hardly depend on the thickness d of the amorphous silicon layer. This is expected because the reflectivity of a-Si films of $d > 0.2\,\mu m$ is not influenced by interference and all power of the green laser coupled in is almost completely absorbed in both films. Furthermore, under the present laser treatment conditions, the heat flow density generated within the a-Si:H films is too low to cause a significant temperature difference (exceeding 10-20 °C) over the a-Si:H film thickness (see Sec. III G). As discussed in Sec. III G, the actual heating of the a-Si:H films is considered to arise by the heat flow from the a-Si:H film into the glass substrate causing a temperature gradient predominantly in a rather thin glass layer (heated glass layer thickness $d_G \ll$ thickness of glass plate) at the glass-amorphous silicon interface.[18,26] This substrate heating process can be characterized by a heating time t_0. If t_0 is equal or exceeding in magnitude the residence time t^*, t^* will limit the heating process so that with rising scan speed (decreasing residence time) the temperature in the laser spot will decrease.[27,30]

We remark that the observed crystallization effects [see Fig. 1(b), Sec. II and Fig. 3, Sec. III B] allow some independent estimation of the laser spot temperature. For example, for glass side illumination and a scan speed of 5 mm/s [Fig. 1(b), field 3.3/v5G, upper left corner], crystallization occurs in sample L24 near a laser power of 3.3 W, with the yellow color of the crystallized material just barely visible. These laser scanning conditions correspond according to Fig. 8 to an extrapolated temperature of $T_{DH} \approx 950$ °C. Data by Blum and Feldman[50] for the relation between crystallization temperature T of amorphous silicon and annealing time t [$t = 5 \times 10^{-14}$ s exp (3.1 eV/kT)] suggest for the residence

time of $t^* = 0.14$ s (corresponding to the scan speed of 5 mm/s) a crystallization temperature of 985 °C, i.e., there is a good agreement. Similarly, the crystallization data (XL) in Fig. 3 agree quite well with the Blum and Feldman formula. For example, for $v = 1$ mm/s ($t^* = 0.7$ s), the threshold power for solid phase crystallization of $P = 2.5$ W in Fig. 3 corresponds according to Eq. (1) to a temperature of $T = 891$ °C, while the Blum and Feldman formula yields 918 °C.

F. Influence of the laser treatment setup

Figure 9 shows the temperatures T_{DH} in the laser spot obtained on sample L24 at a scan speed of 5 mm/s for illumination [see Fig. 1(a)] from the a-Si:H layer side (L), from the glass side (G), as well as from the glass side for an a-Si:H film underneath a silver metal coating (G/Ag). For the SIMS measurements of the D-H profiles under the metal coating, the silver layer was removed. The difference between layer side and glass side illumination can be explained by the different refractive index steps, leading (due to different reflection) to a different effective laser power within the a-Si:H film. For layer side illumination, the difference in refractive index between a-Si:H and air gives rise to a change in laser power (at room temperature) by a factor of roughly 0.58. For glass side illumination, one gets a change in laser power by a factor of 0.72, the multiple reflections in the glass substrate included. Due to the difference in laser power within the a-Si:H material, a change in the slope of the T versus P dependence in Fig. 9 for layer side compared to glass side illumination by a factor of $0.58/0.72 = 0.81$ is expected, if temperature dependences of the refractive indices are neglected. The results give a factor of 0.78, i.e., close to the expected value.
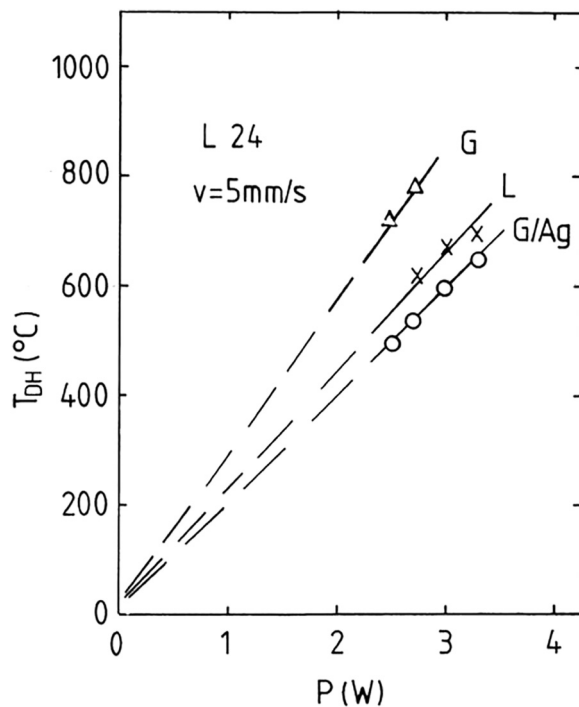
FIG. 9. Temperature T_{DH} in the laser spot as a function of (nominal) laser power P at a scan speed $v = 5$ mm/s for sample L24 at treatment from the a-Si:H layer (L) and glass (G) sides, and at glass side treatment of an a-Si:H film underneath $0.7\,\mu m$ silver metallization (G/Ag).

FIG. 10. Temperature T_{DH} in the laser spot underneath a $0.7\,\mu m$ silver contact film as a function of laser power P (sample L24) for various scan speeds v. Dashed lines indicate extrapolation to $T = 20$ °C for $P = 0$ W.

We associate the observed reduction of T_{DH} underneath the silver contact mainly with lateral heat conduction in the silver film. Accordingly, this reduction is expected to depend on the thickness of the silv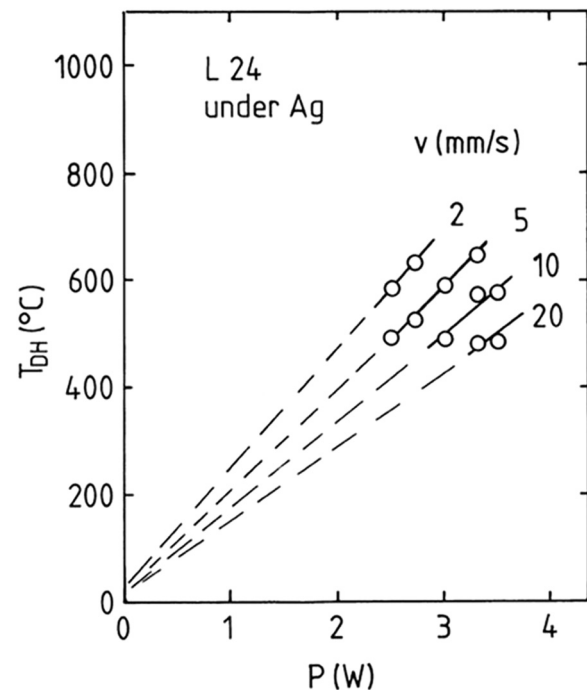er metallization. The present results refer to a thickness of the silver layer of $\approx 0.7 \mu m$ and suggest that the film temperature at the same laser power for a scan speed of 5 mm/s is changed by the factor $F \approx 0.7$.

In Fig. 10, the data points show for sample L24 the temperature T_{DH} below the silver coating for various scan speeds v. The dashed lines indicate the extrapolation to $T = 20\,°C$ for $P = 0$ W. In Fig. 11, the (extrapolated) temperature for a laser power $P = 2$ W is compared for films with and without silver layer as a function of scan speed. It is seen that with increasing scan speed (decreasing temperature), the factor $F = T_{DH}$ (with Ag)/T_{DH} (without Ag) approaches unity. This is expected as with decreasing temperature in the laser spot, the lateral heat flow in the silver layer will decrease, too. In agreement with this concept of lateral heat conduction in the silver layer, we found underneath the silver contacts a dependence on contact size. While underneath the small silver dots in the field 2.5/v2G of Fig. 1(b), a temperature of $655\,°C$ was measured, underneath the broad silver contact stripe in the same field, the temperature was only $580\,°C$.

G. Model for temperature rise in the laser spot and comparison with temperature calculations

The laser light of 532 nm wavelength is almost fully absorbed near the surface of the a-Si:D/a-Si:H double layer (i.e., at a depth $<0.1 \mu m$) and transformed to heat. Neglecting heat dissipation from the layer surface, heat flows primarily from the heated layer volume toward the layer-glass interface. Considering the static case (scan speed $v = 0$), the heat flow

FIG. 11. T_{DH} versus scan speed at $P = 2$ W with and without the silver layer. The factor $F = T_{DH}$ (with Ag)/T_{DH} (without Ag) is shown in the upper part.

across the amorphous layer of thickness d can be considered as quasi-stationary after some initial phase. Fourier's law of heat conduction

$$\Delta T \quad = \quad P^*d/\kappa^*F, \qquad (2)$$

can then be applied (with κ^* being the thermal conductivity of the amorphous Si layer, P^* being the absorbed laser power, and F being the laser spot area) to estimate the laser induced temperature difference ΔT across the amorphous silicon layer. For simplicity, we assume instead of the Gaussian beam intensity profile a constant laser power P^* over the laser spot area F. Using $\kappa^* \approx 1.5$ W/m K of amorphous silicon[59] and the dimensions used in the present experiments $[F = \pi(S/2)^2]$ for a layer thickness of $d \approx 1 \mu m$ (sample L12), a temperature rise of only $\Delta T \approx 10\,°C$ results for a maximum absorbed laser power (glass side) of $P^* \approx 6 \times 0.72$ W (factor 0.72, see Sec. III F). In view of the relatively high experimental temperatures in the laser spot (equal or exceeding $400\,°C$ according to Figs. 8–10) obtained in the present work, we neglect in the following any contribution of heat flow through the amorphous silicon layer to the total temperature rise.

The temperature increase due to heat flow from a static cw laser spot into a substrate material has been calculated by Lax[26] and others.[27,28,60] According to Lax,[26] the maximum temperature rise ΔT_M at a substrate surface due to irradiation with a circular laser spot of Gaussian intensity is given by

$$\Delta T_M^s = P^*/2\pi^{1/2} \kappa r_0. \qquad (3)$$

Here, κ is the heat conductivity in the substrate material, $r_0 = S/2$ is the radius of the laser spot, P^* is the absorbed heat power, and the index s denotes the static irradiation, i.e., zero laser scan speed. Equation (3) is valid for a substrate thickness exceeding greatly the laser spot diameter.[61]

In the dynamic case, the material is continuously heated and later it cools down again as the laser spot moves on. The temperature in the laser spot is proportional to the absorbed energy which in turn is proportional to the exposure time t. Two time periods are involved in the heating process: (i) the heating time t_0 which refers to the static heating and (ii) the laser residence time t^* which relates to the scanning process characterized by the scan velocity $v = 2 r_0/t^*$. If t_0 is small compared to t^*, the substrate surface and thus the amorphous film will heat up to the maximum temperature and the same maximum dynamic and static temperatures are expected. However, if t_0 is of the same order or exceeds t^*, a smaller temperature rise is expected in the dynamic case than in the static one and was found by computer simulation.[30] This is because the laser spot will move on before the static maximum temperature is reached. Thus, in the dynamic case, a reduction of the temperature by the time scaling factor $t^*/(t^* + t_0)$ can be expected, i.e.,

$$\Delta T_M^d = \Delta T_M^s t^*/(t^* + t_0). \qquad (4)$$

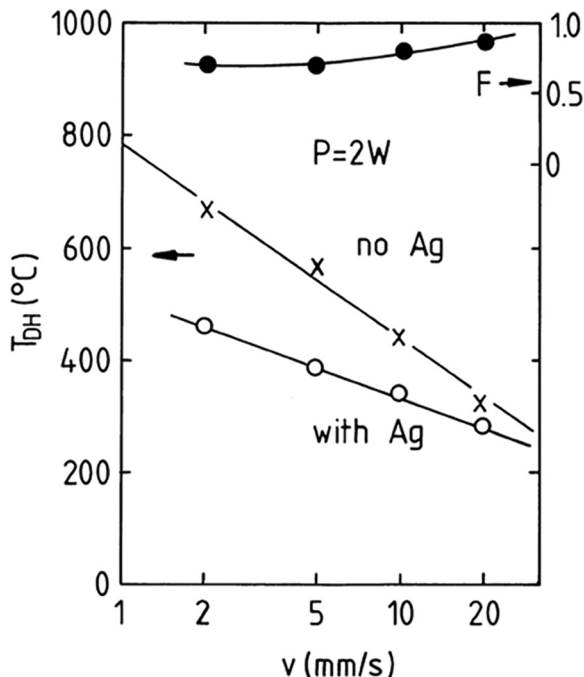Here, the index d indicates the dynamic situation. The maximum temperature rise in the center of a Gaussian laser

spot then follows to

$$\Delta T_M^d = (P^*/\kappa\, 2\pi^{1/2}\, r_0)[t^*/(t^* + t_0)], \tag{5a}$$

and

$$\Delta T_M^d = (P^*/\kappa\, 2\pi^{1/2}\, r_0)(1 + t_0\, v/2\, r_0)^{-1}. \tag{5b}$$

Thus, for the calculation of the temperature rise as a function of residence time t* and scan speed v, knowledge about the heating time t_0 is required. This heating time t_0 describes the characteristic time period for reaching the maximum static temperature. Tonneau *et al.*,[30] e.g., defined it as the time period for reaching 95% of the maximum temperature. For simplicity, we assume ΔT_M^s to be linearly dependent on t_0. Via the expression $L_0 = 2\,(D_S\, t_0)^{1/2}$ (D_S is the heat diffusivity in the substrate material), t_0 is then related to the heat diffusion length L_0 (within the substrate material) which corresponds to the heating of the substrate surface to the maximum static temperature. Setting

$$L_0 = z\, r_0, \tag{6}$$

Equation (5b) becomes

$$\Delta T_M^d \approx (P^*/\kappa\, 2\pi^{1/2}\, r_0)\,(1 + z^2 r_0\, v/8 D_S)^{-1}. \tag{7}$$

In the following, we use z as a free parameter for comparison of Eq. (7) with our experimental data (glass side illumination) of Fig. 8. Assuming various values of z and using the heat diffusivity and heat conductivity data of the employed glass substrates at T = 500 °C ($D_S = 0.00518$ cm²/s and $\kappa = 0.0142$ W/cm °C),[38] the temperature T = ΔT + 20 °C was calculated. A good agreement is found for z ≈ 1, as is demonstrated in Fig. 12.
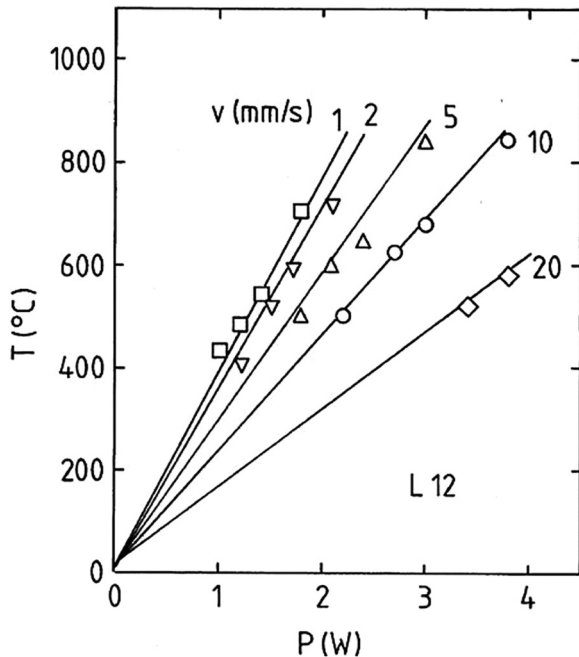
FIG. 12. Temperature T in the laser spot as a function of laser power P for illumination from the glass side on sample L12, calculated according to Eq. (7) using z = 1.0 (lines) and measured by D-H interdiffusion (data points).

Equation (7) has a form similar to Eqs. (15) and (16) of Nissim *et al.*,[28] who solved the heat diffusion equation. They obtain for the temperature rise ΔT_M^d caused by a circular (Gaussian) laser beam

$$\Delta T_M^d = \Theta_{max}\eta = [P(1 - R)/C_p\, D_S\, r_0^N\, 2(2\pi)^{1/2}]\eta. \tag{8}$$

Here, Θ_{max} is the maximum static temperature, η is an integral function depending on laser scan speed, P × R is the reflected laser power, and C_p and D_S are the specific heat and the heat diffusivity, respectively, of the substrate material. Note that the radius of the laser spot in Ref. 28, r_0^N, is differently defined compared to the radius r_0 used in the present work. It is defined by the point where the laser intensity has dropped by the factor $e^{1/2}$ (see Ref. 60), while we define r_0 (see Sec. II) by the point where intensity has dropped by a factor e. Thus,

$$r_0^N = r_0/2^{1/2} \tag{9}$$

and, with P (1−R) = P* and $C_p\, D_S = \kappa$ (see Ref. 26),

$$\Theta_{max} = P^*/\kappa\, r_0\, 2\pi^{1/2} = \Delta T_M^s. \tag{10}$$

The function η is plotted in Fig. 10 of Ref. 28 versus the normalized velocity V which is defined as

$$V = v_N\, r_0^N/2D_S. \tag{11}$$

With

$$v_N = 2r_0^N/t^* = 2r_0/t^*\, 2^{1/2} = v/2^{1/2}, \tag{12}$$

[t* the residence time (see Sec. III A)], Eq. (11) becomes

$$V = v\, r_0/4\, D_S, \tag{13}$$

and Eq. (7) attains the form

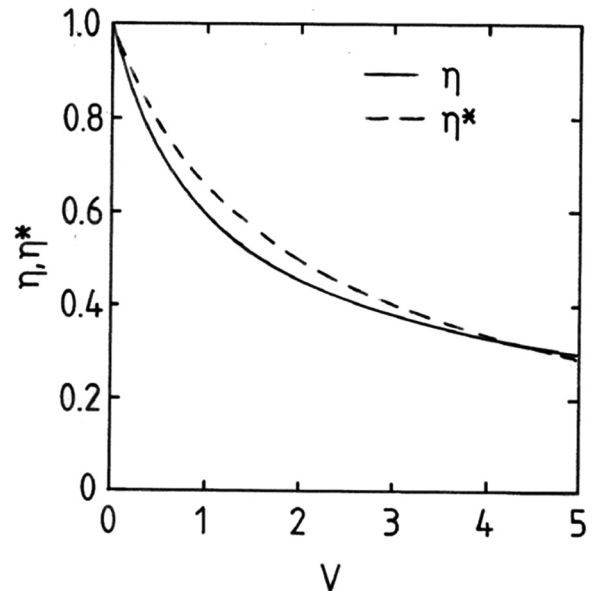$$\Delta T_M^d = (P^*/\kappa\, r_0\, 2\pi^{1/2})\,(1 + z^2V/2)^{-1}. \tag{14}$$

FIG. 13. Functions η of Ref. 28 and η* [Eq. (15) with z = 1] versus normalized velocity V defined by Eqs. (11) and (13).

A comparison of Eq. (14) with Eqs. (8) and (10) then shows that the function

$$\eta^* = 1/(1 + z^2 V/2), \tag{15}$$

is an analytic approximation of the integral function η of Ref. 28. In Fig. 13, η^* is plotted as a function of V, assuming $z = 1$. η as a function of V is also shown in Fig. 13, taken from Fig. 10 of Ref. 28. As shown, η^* and η agree for $V = 0$ and $V \approx 4$, while some deviations occur at $0 < V < 4$ and $V > 4$. Presumably, these deviations are caused by inaccuracies in our estimation of t_0.

In Fig. 14, we compare for a laser power of $P = 2W$, applied from the glass side (extrapolated), experimental and calculated temperature values as a function of laser scan speed v. The experimental temperature values for D-H interdiffusion were taken from Fig. 8 and those by melting point analysis were determined according to Eq. (1). Calculated data points are based on the work of Cline and Anthony[27] and Nissim *et al.*[28] taking into account the different definitions of the laser spot radius as explained above. For all calculations, $P^* = 0.72\, P$ was used accounting for reflection losses (see Sec. III F). Temperature values calculated according to Eq. (7), using $z = 1.0$, are also shown. The results show that most experimental data as well as the calculated data by Cline and Anthony,[27] by Nissim *et al.*,[28] and by the approximation formula Eq. (7) lie close together. We consider this result as a remarkable agreement between calculation and experiment.

Table I gives an overview of the assumptions involved in the methods for temperature characterization in the laser spot applied in this article. Accordingly, all methods used involve assumptions and/or simplifications. The close agreement of the data in Fig. 14 shows, however, that the assumptions made are not completely wrong and/or are not of decisive importance for the final result.
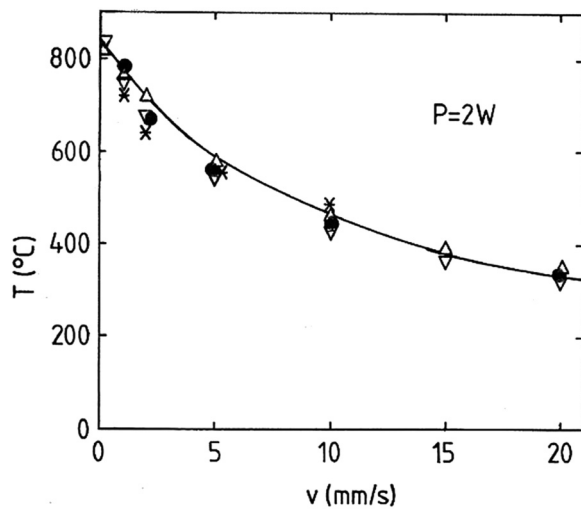
The results of Fig. 14 demonstrate, furthermore, that for the simple laser heating setup (single film on the substrate, optimized film-substrate interface, scanning by a cw Gaussian laser beam which is fully absorbed), various choices for characterization of the temperature in the laser spot (besides the D-H interdiffusion method) exist, the most simple being the temperature calculations based on data by Cline and Anthony[27] and Nissim *et al.*[28] or the approximation by Eq. (7), all needing appropriate input parameters. Note, furthermore, that once the melting point analysis has been performed for a specific a-Si:H film, Eq. (1) is a convenient way to determine the temperature in the laser spot for various other a-Si:H films of similar deposition conditions.

H. Advantages and limitations of the D-H interdiffusion method for temperature measurements in the laser spot

While the D-H interdiffusion method gives for the simple laser annealing setup according to Fig. 14 similar results for the temperature in the laser spot as the other methods and can be very useful for improvement of film-substrate interfaces (see Table I and Sec. I), its strength lies in the application for temperature measurements in multilayers, as is demonstrated for silver overlayers in Sec. III F. In this case, the temperature rise cannot simply be calculated. If precise experimental temperature and H diffusion data for laser and RTP treatment of a-Si:H-based multilayers are required, we consider the D-H method superior to any other laser spot temperature measurement known to us so far, by several reasons. Namely, (i) the heat flow is not disturbed by measurements, as, e.g., by use of thermocouples, (ii) both H diffusion length and temperature data are obtained, (iii) the temperature is measured within the films, i.e., unaffected by optical emission factors like it is the case for the pyrometer or thermal imaging camera, (iv) even depth resolution is possible by placing D/H junctions at various depths, and (v) due to SIMS depth profiling any irregularities like poor interfaces, film microstructure, contact material diffusion, and metal-induced crystallization are readily detected.

FIG. 14. Temperature T in the laser spot for a simple setup at $P = 2W$ (glass-side illumination) as a function of laser scan speed v. Experimental data by D-H interdiffusion (●) (Fig. 8, sample L12) and by melting point analysis (*). Calculated data points from publications by Cline and Anthony[27] (△) and Nissim *et al.*[28] (▽). Full line was calculated according to Eq. (7) using $z = 1.0$.

TABLE I. Assumptions involved in the applied methods for characterization of temperature in the laser spot.

Assumption	D-H interdiff.	Melting point	Calculation Eq. (7)	Calc.[27,28]
Constant refract. index at $T \geq 20\,°C$	No	Yes	Yes	Yes
Annealing time $t = t^*$	Yes	No	Yes	Yes
ΔT and P^* linear dependent	No	Yes	Yes	Yes
Literature data for κ and D_S	No	No	Yes	Yes
Well-defined film-substrate interface	No	Yes	Yes	Yes
Value for z ($z = 1$)	No	No	Yes	No
High T hydrogen diff. parameters	Yes	No	No	No

The D-H interdiffusion method has, however, some limitations which lie, e.g., in the necessity of dense a-Si:H (with steep Arrhenius-dependence of H diffusion, see Sec. I). Furthermore, a rather smooth substrate, a minimum thickness of the D/H layers, and a minimum temperature in the laser spot are required for precise evaluation of the H diffusion length using SIMS. Also, the high temperature H diffusion parameters used in this article (Sec. III A) may not be generally valid and may need an adjustment. A way to measure the high temperature H diffusion parameters is described in Sec. III I.

I. Application of laser scanning induced D-H interdiffusion for measurement of high temperature hydrogen diffusion coefficient

Hydrogen diffusion measurements by D-H interdiffusion using furnace annealing are usually limited to temperatures ≤500 °C because of a-Si crystallization. Moreover, the annealing time typically used for furnace annealing of $t \geq 5$ min causes in a-Si:H at $T \geq 550$ °C large H diffusion lengths leading for film thicknesses ≤1 μm to a reduction in the accuracy of error-function fitting and to significant H outdiffusion. To our knowledge, no experimental data on the temperature dependence of the (D-H interdiffusion based) H diffusion coefficient of a-Si:H at $T > 500$ °C have been published so far. By application of laser scanning, H diffusion measurements can be extended considerably beyond 500 °C due to the application of a much shorter annealing time which shifts up the crystallization temperature[37,50] and reduces H outdiffusion. While the H diffusion coefficient in the laser spot is obtained from the measured H diffusion

length and the laser residence time (see Sec. III A), the temperature in the laser spot needs to be defined otherwise, e.g., by temperature calculation or by application of the melting point method using a simple laser scanning (single film on substrate) setup. Thus, D-H interdiffusion induced by laser scanning can be used to determine the high temperature hydrogen diffusion parameters without relying on model assumptions.

In Fig. 15, the data points show the H diffusion coefficient D in sample L12 determined from the D-H interdiffusion for various laser scan speed (residence time) and laser power values as a function of 1/T. The temperature was taken from calculations by Cline and Anthony[27] using literature data at $T = 500$ °C for the heat propagation parameters D_S and κ of the substrate material.[38] As it is seen, the maximum hydrogen diffusion temperature exceeds the maximum furnace annealing temperature of approximately 500 °C[35] by more than 300 °C. The straight line obtained by linear regression gives the Arrhenius dependence $D = 4 \times 10^{-4}$ cm^2 s^{-1} exp(-1.33 eV/kT). This experimentally determined temperature dependence is in close agreement (within experimental error) with the high temperature Arrhenius dependence of H diffusion [$D = 10^{-3}$ cm^2 s^{-1} exp(-1.39 eV/kT)] based on the Meyer-Neldel rule and the theoretical H diffusion prefactor D_0^T in silicon (see Sec. III A), used in this article to calculate the temperature in the laser spot. Thus, for the present device grade a-Si:H material, the validity of the used H diffusion parameters for high temperatures is confirmed as expected by the general agreement of the D-H interdiffusion-based temperatures with the data derived by the other applied methods (see Figs. 5 and 14).

Apart from different Arrhenius parameters, low temperature H diffusion at $T < 500$ °C $\approx T^{MN}$ (measured using furnace annealing) and high temperature H diffusion at $T > 500$ °C (measured using laser scanning) in device-grade a-Si:H ($\approx$15 at. % H) differ also otherwise, namely, by a strong time-dependence in the first case[35] and no detectable time-dependence of the H diffusion coefficient in the latter.[37] Our results for sample L12, involving a variation of scan speed/annealing time by a factor of 10 (see Fig. 4), show at $T > 500$ °C no significant time-dependence of the H diffusion coefficient either, while (using furnace annealing) a strong time-dependence of the H diffusion coefficient at $T < T^{MN}$ was confirmed. Several models have been proposed to explain the time-dependence of the H diffusion coefficient in a-Si:H, like hydrogen motion by a multiple trapping process,[63] and the drop of the hydrogen chemical potential due to H outdiffusion into voids[35,36] or due to non-equilibrium.[35] We note that the different time-dependences of H diffusion at T below and above the Meyer-Neldel temperature point for the present material against both a (simple) multiple trapping model and H outdiffusion into voids, but appear to be consistent with the model of H diffusion at non-equilibrium conditions at $T < T^{MN}$ and equilibrium conditions at T equal or exceeding the Meyer-Neldel temperature.[35,36,62] A model invoking a transition from extrinsic to intrinsic transport for the explanation of Meyer-Neldel dependences was recently discussed in detail by Widenhorn *et al.*[64] The explanations of Meyer-Neldel dependences by

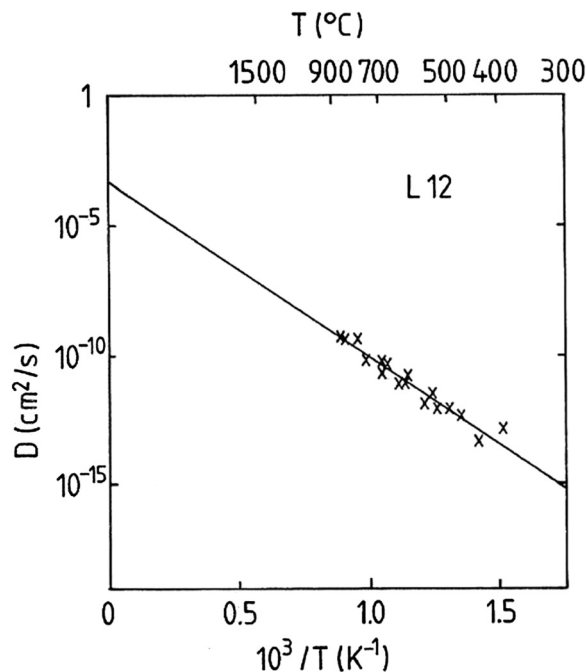FIG. 15. Hydrogen diffusion coefficient D in sample L12 as a function of 1/T. D was determined by deuterium-hydrogen interdiffusion, 1/T was obtained by calculation[27] using D_S and κ literature data at $T = 500$ °C.[38] The full line indicates the linear regression of the data points with a diffusion prefactor of $D_0 = 4 \times 10^{-4}$ cm^2/s and a diffusion energy of $E_D \approx 1.33$ eV.

Beyer[35,36] and Widenhorn *et al.*[64] differ considerably from previous models by, e.g., Khait *et al.*[65] and Yelon *et al.*[66] who attributed the observation of Meyer-Neldel dependences to activation processes involving multiphonon excitations. Different predicted (1/T)-dependences below and above the Meyer-Neldel temperature may be used as a distinction. While the models by Refs. 65, 66 predict a crossover, the models by Ref. 35 (see Sec. III A) and Ref. 64 predict a convergence into a single dependence at $T > T^{MN}$. While little experimental data measured at temperatures $T > T^{MN}$ exist so far,[64,67] our technique of high temperature H diffusion measurements based on laser scanning opens the possibility to obtain such data for various a-Si:H materials. Our first results for device-grade a-Si:H point against a crossover, since $E_D \approx 1.33\,eV$ is obtained at $T > T^{MN}$ (see Fig. 15), while at $T < T^{MN}$ for this material $E_D = 1.25\,eV$[35] is valid. In addition, there is a time dependence of H diffusion only at $T < T^{MN}$, not at $T > T^{MN}$, as mentioned above. More measurements in particular on samples with strongly different H concentration would be useful, however, for a firm assignment. The understanding of Meyer-Neldel rules (in general) is of great general scientific interest. The understanding of the (specific) Meyer-Neldel rule and of the time-dependence of hydrogen diffusion in a-Si:H could greatly contribute to a better knowledge of the role of hydrogen in thin film silicon[62] and even in hydrogenated crystalline silicon. Recent measurements of hydrogen outdiffusion from proton-implanted crystalline silicon (Ref. 68) show a qualitatively similar correlation between H diffusion prefactor and H diffusion energy as observed for a-Si:H.[35,36] Only the hydrogen diffusion energy in hydrogenated crystalline silicon comes out to be smaller than in a-Si:H for the same H diffusion prefactors.

J. Application of temperature controlled rapid thermal processing (including laser annealing) in a-Si:H technology

Hydrogenated amorphous silicon being an abundant non-toxic semiconductor material compatible with glass and plastics as a substrate, a wide range of applications for this material, involving various annealing procedures, are conceivable and have been studied and applied in the past 50 years. For example, in the years near 1980, laser annealing of a-Si:H was investigated for use in optical recording.[18,69] At present, the major commercial products based on hydrogenated amorphous silicon are thin film transistors for large area displays and solar cells. In these production fields, several applications of rapid thermal processing/laser annealing are already applied, in discussion or conceivable like the realization of a-Si:H of reduced hydrogen content as a starting material for crystallization, the implementation of high temperature (reaction or diffusion) processes involving a-Si:H, and the use of a-Si:H as a source of hydrogen. In all three cases, the process time is/could be greatly reduced by RTP/laser heating compared to furnace annealing. Additional advantages of RTP/laser annealing (compared to furnace annealing) arise from a confinement of heating to surface layers making possible depth-dependent heating,[11] treatment of individual layers,[17] and spatially-resolved annealing.[16,17]

A better control of annealing temperature or of hydrogen diffusion length in these production process steps could be of high impact. Furthermore, temperature controlled RTP/laser annealing may lead to an improvement of the a-Si:H material itself.

The challenge for fabrication of a-Si:H of reduced H concentration by laser annealing lies in the fact that the thresholds for dehydrogenation (photo-darkening[18]) and of (solid phase) crystallization lie fairly close together (see Fig. 3). Thus, for dehydrogenation without crystallization, a temperature control (like by the D-H interdiffusion method) appears indispensable. High temperature processes involving hydrogenated amorphous silicon include, e.g., metal-induced crystallization, silicide formation, and impurity atom diffusion.[70] In all cases, knowledge of precise temperature is required. For generating a defined flow of hydrogen at a given temperature, a temperature control appears also to be necessary. By the choice of material and temperature, specific flows of H atoms and H_2 molecules can be generated.[36] In silicon heterojunction technology, such flows of hydrogen are used to passivate defects at the crystalline silicon surface.[3]

For the reduction of defect concentration in the a-Si:H material (e.g., defects arising from deposition process, illumination, or bias stress) by annealing, it appears necessary to minimize H outdiffusion, a process which may generate silicon dangling bonds. Again, a strict control of temperature/H diffusion length is necessary, as discussed in Sec. III K. For H-diffusion based annealing processes which are generally assumed for a-Si:H,[48] one may expect for the same annealing-related H diffusion length the same structural or optoelectronic changes of the material (independent of annealing temperature/annealing time) as long as the material does not crystallize. However, it is known that defect generation in a-Si:H (in particular by light absorption) involves defects created not just by rupture of Si-H bonds which may readily be restored by H diffusion, but also by rupture of Si-Si bonds[71] which may not necessarily be restored by H diffusion. Thus, it is conceivable that fixed H diffusion length annealing may have a somewhat different impact on structural and optoelectronic properties when done at high or low temperatures. More work of defect annealing at various temperatures appears necessary and the present article may provide a basis.

Several studies of structural and optoelectronic changes of (dense) a-Si:H by H outdiffusion exist, based on furnace annealing experiments performed at $T \le 500\,^\circ C$.[37,56,72–74] Conspicuous effects caused by H release are the reduction of the optical bandgap of a-Si:H,[73] the generation of microvoids[73,74] and of Si dangling bond related defects.[75] For H outdiffusion by laser scanning, similar annealing effects as for furnace annealing are expected to occur for the same H diffusion lengths, but due to the much shorter annealing time periods much higher annealing temperatures are required. First results for annealing of a-Si:H films on crystalline silicon substrates by both furnace and laser annealing[37] indeed show clear similarities in the evolution of (void-related) microstructure for furnace and laser annealing when similar quantities of hydrogen are released at completely different

annealing time/annealing temperature scales (e.g., 5 min/500 °C furnace annealing corresponds roughly to 10 ms/900°C laser annealing). For the high temperature laser annealing, our results of Sec. III D support the importance of the H diffusion length for the characterization of the annealing state by the correlation between the photo-darkening effect and the H diffusion length. While void and Si dangling bond formation are usually considered deleterious to the material quality, we note that (in particular if partial local crystallization is involved) nanostructured silicon materials[76] with different bandgaps may also get produced by laser scanning, i.e., materials of high scientific and technological interest. By application of laser scanning, such materials may be fabricated with precise temperature control even underneath metal or transparent conducting oxide contacts as well as spatially resolved. Note that the laser-based D-H interdiffusion method allows spatially resolved temperature and H diffusion-length measurements, as modern SIMS analysis tools permit a rather high spatial resolution.[77]

K. Hydrogen diffusion length for defect annealing

For the application of laser annealing to a-Si:H based solar cells aiming for H diffusion based defect reduction, the measurement of H diffusion length within the a-Si:H films is of interest, in particular below metal layers since solar cells usually have metal contacts. In Fig. 16, the H diffusion length L (obtained directly from D-H interdiffusion) is shown as a function of laser scan speed v at various levels of laser power P for annealing from the glass side underneath the $0.7 \mu m$ thick silver layer. The H diffusion length L is
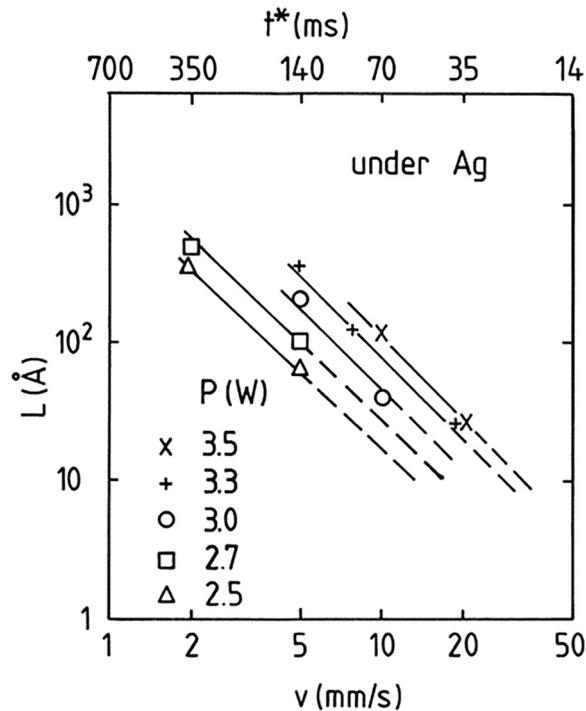

FIG. 16. H diffusion length L of a-Si:H (sample L24) underneath silver metallization as a function of laser scan speed v and residence time t* for various nominal laser power (P) values. Dashed lines indicate extrapolation of laser scan parameters into the L ≤ 10 Å range.

seen to increase quite strongly with decreasing scan speed v and increasing residence time t*. Roughly, L is proportional to t^{*2}. Two components contribute to this dependence according to the relation $L = 2 (D t^*)^{1/2}$, the explicit square root time dependence of the diffusion length and the increase of the H diffusion coefficient D with rising residence time, as the latter causes at fixed laser power an increase of temperature in the laser spot.

The choice for an optimum H diffusion length for defect annealing in a-Si:H needs to consider two aspects: on one hand, the H diffusion length should be as short as possible to minimize H outdiffusion from the a-Si:H film, as this process is expected to generate defects.[75] On the other hand, the H diffusion length should be long enough for diffusing H to reach any defect in the amorphous silicon. We estimate this latter length by the mean distance of two incorporated hydrogen atoms from each other. For example, for 15 at. % H concentration in a-Si:H, one gets an average distance of roughly 6 Å. Thus, we expect improvement of the a-Si:H material at diffusion lengths in the range of 1-10 Å. The results in Fig. 16 demonstrate that an extrapolation of the laser scan parameters to obtain H diffusion lengths of 1-10 Å is possible.

It needs to be noted, however, that for achieving rather precise H diffusion lengths by extrapolation, the involved annealing temperature should always be equal or exceed the Meyer-Neldel temperature $T^{MN} \approx 500$ °C. For laser spot temperatures T below T^{MN}, the high temperature H diffusion parameters are no longer (strictly) valid and a time-dependence of the H diffusion coefficient (see Sec. III I) shows up, which is particularly strong for device-grade a-Si:H with hydrogen concentrations near 15 at. %.[35] Thus, laser annealing conditions with a fairly high laser power at rather a high scan speed are expected to lead to more precise H diffusion lengths. We note, furthermore, that in particular for precise laser annealing aiming to reduce the defect concentration, a more homogeneous laser treatment is required than the one employed in the present work. Since a Gaussian intensity profile along with the fairly big line offset equal to the laser spot radius was applied (see Sec. II), a variation of laser power in the direction perpendicular to laser scanning exceeding 20% and a corresponding variation in annealing temperature must be expected. A much shorter line offset (i.e., multiple overlapping scans) or a flat-top laser intensity profile appears necessary.

IV. CONCLUSIONS

The extensive comparison of data for the temperature in the laser spot based on SIMS depth profiling of D/H layer samples with temperature data obtained otherwise shows a high degree of agreement which implies that high temperature H diffusion parameters for D-H interdiffusion based on a recent model are valid for the device-grade (dense) a-Si:H investigated. The high potential for precise measurements of temperatures exceeding 500 °C by the D-H interdiffusion method is demonstrated and inherent advantages like its insensitivity to the substrate material and to interface quality are pointed out. Effects of photo-darkening in a-Si:H are

elucidated, and the dependence of the photo-darkening effect on the H diffusion length is confirmed. The temperature underneath metal contact layers can be determined by the D-H interdiffusion method and is found to be reduced compared to the case without metal overlayer, depending on temperature. The data of the hydrogen diffusion length, measured underneath metal contacts as a function of laser scan speed and laser power allow an extrapolation of laser parameters to reach H diffusion lengths in the range of 1-10 Å for which improvements of a-Si:H material properties by diffusing H can be expected. Thus, based on the current understanding of H diffusion in a-Si:H, D-H interdiffusion can provide a versatile tool for precise characterization of rapid annealing processes, and well-controlled (with regard to temperature and H diffusion length) laser annealing of a-Si:H films and multilayers at temperatures below a-Si crystallization appears possible. Annealing effects for constant H diffusion length and different laser spot temperature can be studied. Applications may lead to a reduction of annealing-related process time and to the realization of new device options in the field of solar cells and large area displays. Furthermore, it is demonstrated that laser annealing (involving a short annealing time) in combination with temperature calculations or other methods of temperature reading can be used to measure the H diffusion coefficient for D-H interdiffusion in a-Si:H at temperatures exceeding $T = 500\,^\circ C$, i.e., in a temperature range inaccessible so far. The experimental results confirm the model-based high temperature H diffusion Arrhenius parameters and support by new information on the time-dependence of H diffusion in a-Si:H a recent model explaining the Meyer-Neldel dependence of hydrogen diffusion in a-Si:H by a transition from non-equilibrium to equilibrium situations. Thus, based on the improved understanding of laser annealing provided in this study, an improved knowledge about the role of hydrogen in amorphous silicon is obtained. We note, furthermore, that high temperature H diffusion measurements based on laser scanning of various types of a-Si:H (and of related materials) may provide the possibility of testing models explaining the experimental Meyer-Neldel dependence observed in the $T \leq 500\,^\circ C$ range.

ACKNOWLEDGMENTS

NOMENCLATURE

D_S	Heat diffusivity in substrate material
L	Diffusion length (both heat and hydrogen)
P	Laser power applied
P^*	Heat power inside material (related to absorbed laser power)
PD	Photo-darkening
r_0	Radius of laser spot
S	Diameter of the laser spot
SPD	Standard photo-darkening
t^*	Laser residence time
t_0	Heating time
T_{DH}	Laser spot temperature determined by D-H interdiffusion
T_{MP}	Laser spot temperature determined by silicon melting point analysis
v	Laser scan velocity
z	Heat diffusion length in multiples of r_0
ΔT	Temperature rise
ΔT_M^d	Maximum dynamic ($v \geq 0$) temperature rise
ΔT_M^s	Maximum static ($v = 0$) temperature rise
κ^*	Heat conductivity in a-Si:H
κ	Heat conductivity in the substrate material

[1] D. L. Staebler and C. R. Wronski, Appl. Phys. Lett. **31**, 292 (1977).

[2] K. Wilken, F. Finger, and V. Smirnov, Energy Proc. **84**, 17 (2015).

[3] S. De Wolf, A. Descoeudres, Z. C. Holman, and C. Ballif, Green **2**, 7 (2012).

[4] J. Schmidt and A. Cuevas, *Proceedings of 16th European Photovoltaic Solar Energy Conference* (James & James, London, 2000), p. 1193.

[5] P. Mei, J. B. Boyce, M. Hack, R. A. Lujan, R. I. Johnson, G. B. Anderson, D. K. Fork, S. E. Ready, and D. L. Smith, Mater. Res. Soc. Symp. Proc. **297**, 151 (1993).

[6] W. S. Ryu, S. Y. Sung, W. J. Chang, J. Kang, K. S. Cho, S. M. Seo, W. S. Son, J. I. Lee, K. S. Park, K. T. Lee, S. R. Lee, and W. H. Cho, *Proceedings AM-FPD 17*, Kyoto, Japan, 4–7 July 2017, p. 157.

[7] Y. C. Jung, S. Seong, T. Lee, J. Ahn, T. H. Kim, W. J. Yeo, and I. S. Park, Semicond. Sci. Technol. **32**, 025007 (2017).

[8] S. J. Park, Y. M. Ku, K. H. Kim, E. H. Kim, B. K. Choo, J. S. Choi, S. H. Kang, Y. J. Lim, and J. Jang, Thin Solid Films **511**, 243 (2006).

[9] J. B. Boyce and P. Mei, in *Technology and Applications of Amorphous Silicon*, edited by R. A. Street (Springer, Berlin, 2000), p. 94.

[10] J. G. Maillou, E. L. Mathé, J. C. Desoyer, S. De Unamuno, and E. Fogarassy, Appl. Surf. Sci. **43**, 150 (1989).

[11] K. Sera, F. Okumura, H. Uchida, S. Itoh, S. Kaneko, and K. Hotta, IEEE Trans. Electron Devices **36**, 2868 (1989).

[12] D. Toet, P. M. Smith, T. W. Sigmon, T. Takehara, C. C. Tsai, W. R. Harshberger, and T. O. Thompson, J. Appl. Phys. **85**, 7914 (1999).

[13] N. H. Nickel, in *Laser Crystallization of Silicon*, edited by N. H. Nickel, Semiconductors and Semimetals Vol. 75 (Elsevier, Amsterdam, 2003), p. 1.

[14] P. Lengsfeld, N. H. Nickel, and W. Fuhs, Appl. Phys. Lett. **76**, 1680 (2000).

[15] J. Haschke, D. Amkreutz, and B. Rech, Jpn. J. Appl. Phys. **55**, 04EA04 (2016).

[16] P. Mei, J. B. Boyce, M. Hack, R. A. Lujan, R. I. Johnson, G. B. Anderson, D. K. Fork, and S. E. Ready, Appl. Phys. Lett. **64**, 1132 (1994).

[17] P. Mei, J. B. Boyce, M. Hack, R. Lujan, S. E. Ready, D. K. Fork, R. I. Johnson, and G. B. Anderson, J. Appl. Phys. **76**, 3194 (1994).

[18] D. L. Staebler, J. Appl. Phys. **50**, 3648 (1979).

[19] J. S. Yun, C. H. Ahn, M. Jung, J. Huang, K. H. Kim, S. Varlamov, and M. Green, EPJ Photovoltaics **5**, 55204 (2014).

[20] S. K. Lee, C. H. Oh, Y. S. Kim, J. S. Park, and M. K. Han, Mater. Res. Soc. Symp. Proc. **297**, 919 (1993).

[21] A. Chowdhury, A. Bahouka, S. Steffens, J. Schneider, J. Dore, F. Mermet, and A. Slaoui, EPJ Photovoltaics **4**, 45108 (2013).

[22] A. Doolittle, see http://alan.ece.gatech.edu/ECE6450/Lectures/ECE6450L6-Rapid%20Thermal%20Processing.pdf for Rapid Thermal Processing, retrieved February 9, 2018, 23.00 h.

[23] T. O. Sedgewick, Appl. Phys. Lett. **39**, 254 (1981).

[24] T. T. Kodas, T. H. Baum, and P. B. Comita, J. Appl. Phys. **61**, 2749 (1987).

[25] H. S. Carslaw and J. C. Jaeger, *Conduction of Heat in Solids* (Oxford University Press, Oxford, 1959).

[26] M. Lax, J. Appl. Phys. **48**, 3919 (1977).

[27] H. E. Cline and T. R. Anthony, J. Appl. Phys. **48**, 3895 (1977).

[28] Y. I. Nissim, A. Lietoila, R. B. Gold, and J. F. Gibbons, J. Appl. Phys. **51**, 274 (1980).

[29] P. Majumdar and H. Xia, Appl. Math. Model. **31**, 1186 (2007).

[30] D. Tonneau and G. Auvert, Mater. Res. Soc. Symp. Proc. **101**, 131 (1987).
[31] T. Schmidt, A. Gawlik, H. Schneidewind, A. Ihring, G. Andrä, and F. Falk, Opt. Express **21**, 16296 (2013).
[32] R. J. Anderson, J. Appl. Phys. **64**, 6639 (1988).
[33] H. Shanks, C. J. Fang, L. Ley, M. Cardona, F. J. Demond, and S. Kalbitzer, Phys. Status Solidi **100**, 43 (1980).
[34] J. Gope, S. Kumar, A. Parashar, S. Dayal, C. M. S. Rauthan, and P. C. Srivastava, ISRN Nanomater. **2012**, 429348 (2012).
[35] W. Beyer, in *Hydrogen in Semiconductors II*, edited by N. H. Nickel, Semiconductors and Semimetals Vol. 61 (Academic Press, San Diego, 1999), p. 165.
[36] W. Beyer, Sol. Energy Mater. Solar Cells **78**, 235 (2003).
[37] W. Beyer, J. Bergmann, U. Breuer, F. Finger, A. Lambertz, T. Merdzhanova, N. H. Nickel, F. Pennartz, T. Schmidt, and U. Zastrow, Mater. Res. Soc. Symp. Proc. **1770**, 1 (2015).
[38] See https://www.corning.com/media/worldwide/cdt/documents/EAGLE%20XG%20%C2%AE%20Slim%20Glass.pdf for Corning Display Technologies/EAGLE XG Slim/Product Information Sheet/August 2013, retrieved February 10, 2018, 21.30 h.
[39] W. Beyer, P. Hapke, and U. Zastrow, Mater. Res. Soc. Symp. Proc. **467**, 343 (1997).
[40] W. Beyer and U. Zastrow, J. Non-Cryst. Solids **266–269**, 206 (2000).
[41] W. Beyer, J. Herion, H. Wagner, and U. Zastrow, Philos. Mag. B **63**, 269 (1991).
[42] W. Beyer, J. Non-Cryst. Solids **198–200**, 40 (1996).
[43] H. Schmidt, W. Gruber, G. Borchardt, M. Bruns, M. Rudolphi, and H. Baumann, J. Phys. Condens. Matter **16**, 4233 (2004).
[44] W. M. Arnoldbik, C. H. M. Marée, A. J. H. Maas, M. J. van den Boogaard, F. H. P. M. Habraken, and A. E. T. Kuiper, Phys. Rev. B **48**, 5444 (1993).
[45] W. Beyer, U. Breuer, F. Hamelmann, J. Hüpkes, A. Stärk, H. Stiebig, and U. Zastrow, Mater. Res. Soc. Symp. Proc. **1165**, 209 (2009).
[46] D. Tonneau, G. Auvert, and Y. Pauleau, Thin Solid Films **155**, 75 (1987).
[47] W. Beyer, J. Stuke, and H. Wagner, Phys. Status Solidi A **30**, 231 (1975).
[48] R. A. Street, Physica B **170**, 69 (1991).
[49] W. Beyer and H. Wagner, J. Appl. Phys. **53**, 8745 (1982).
[50] N. A. Blum and C. Feldman, J. Non-Cryst. Solids **11**, 242 (1972).
[51] A. Lambertz, F. Finger, R. E. I. Schropp, U. Rau, and V. Smirnov, Progr. Photovolt. Res. Appl. **23**, 939 (2015).
[52] D. E. Carlson and C. W. Magee, Appl. Phys. Lett. **33**, 81 (1978).
[53] Z. Iqbal and S. Vepřek, J. Phys. C: Solid State Phys. **15**, 377 (1982).
[54] J. Shinar, R. Shinar, X. L. Wu, S. Mitra, and R. F. Girvan, Phys. Rev. B **43**, 1631 (1991).

[55] P. V. Santos, N. M. Johnson, and R. A. Street, Phys. Rev. Lett. **67**, 2686 (1991).
[56] C. Ance, F. De Chelle, and J. P. Ferraton, J. Non-Cryst. Solids **91**, 243 (1987).
[57] C. Maurer, S. Haas, W. Beyer, F. C. Maier, U. Zastrow, M. Hülsbeck, U. Breuer, and U. Rau, Thin Solid Films **653**, 223 (2018).
[58] M. Reinelt, S. Kalbitzer, and G. Müller, J. Non-Cryst. Solids **59-60**, 169 (1983).
[59] D. G. Cahill, M. Katiyar, and J. R. Abelson, Phys. Rev. B **50**, 6077 (1994).
[60] J. E. Moody and R. H. Hendel, J. Appl. Phys. **53**, 4364 (1982).
[61] M. Sparks, J. Appl. Phys. **47**, 837 (1976).
[62] W. Beyer, Phys. Status Solidi A **213**, 1661 (2016).
[63] R. A. Street, C. C. Tsai, J. Kakalios, and W. B. Jackson, Philos. Mag. B**56**, 305 (1987).
[64] R. Widenhorn, A. Rest, and E. Bodegom, J. Appl. Phys. **91**, 6524 (2002).
[65] Y. L. Khait, R. Weil, R. Beserman, W. Beyer, and H. Wagner, Phys. Rev. B **42**, 9000 (1990).
[66] A. Yelon, B. Movaghar, and H. M. Branz, Phys. Rev. B**46**, 12244 (1992).
[67] R. Widenhorn, L. Mündermann, A. Rest, and E. Bodegom, J. Appl. Phys. **89**, 8179 (2001).
[68] M. Faccinelli, S. Kirnstoetter, M. Jelinek, T. Wuebben, J. G. Laven, H. J. Schulze, and P. Hadley, e-print arXiv:1611.04312v3 [cond-mat.mtrl-sci] (2016).
[69] M. A. Bosch, in *Hydrogenated Amorphous Silicon*, edited by J. I. Pankove, Semiconductors and Semimetals Vol. 21D (Academic Press, Orlando, 1984), p. 173.
[70] H. Stiebig, F. Siebke, W. Beyer, C. Beneking, R. Rech, and H. Wagner, Sol. Energy Mater. Solar Cells **48**, 351 (1997).
[71] M. Stutzmann, W. B. Jackson, and C. C. Tsai, Phys. Rev. B **32**, 23 (985).
[72] T. Hamasaki, M. Ueda, A. Chayahara, M. Hirose, and Y. Osaka, Jpn. J. Appl. Phys. **23**, L81 (1984).
[73] M. Schouten, M.S. thesis, TU Delft, 2013.
[74] W. Beyer, W. Hilgers, D. Lennartz, F. C. Maier, N. H. Nickel, F. Pennartz, and P. Prunici, Mater. Res. Soc. Symp. Proc. **1666** (2014).
[75] D. K. Biegelsen, R. A. Street, C. C. Tsai, and J. C. Knights, Phys. Rev. B **20**, 4839 (1979).
[76] P. Roca I Cabarrocas, A. Fontcuberta I Morral, and Y. Poissant, Thin Solid Films **403**, 39 (2002).
[77] M. Kubicek, G. H. Holzlechner, A. K. Opitz, S. Larisegger, H. Hutter, and J. Fleig, Appl. Surf. Sci. **289**, 407 (2014).